Journal of Basics and Applied Sciences Research (JOBASR)
ISSN print: 3026-9091
Volume 2(1) March 2024
DOI: https://doi.org/10.33003/jobasr-2024-v2i1-25

Analyzing Global Stability of M-Pox Disease Dynamics: Mathematical Insights into Detection and Treatment Strategies

Olopade I. A. [1]*, Akinwumi, T. O. [2], Philemon M. E. [1], Mohammed I. T. [3], Sangoniyi S. O. [4], Adeniran G. A. [5], Ajao S. O. [2], Bello B. O. [6] and Adesanya A. O. [2]

[1]Department of Mathematics and Statistics, Federal University Wukari, PMB 1020, Taraba State, Nigeria.
[2] Department of Mathematics and Computer Science, Elizade University, Ondo State, Nigeria
[3]Department of Mathematics and social sciences, Osun state polytechnic Iree. Nigeria.
[4]Department of Mathematics and Computing Science Education, Emmanuel Alayande University of Education, Oyo, Oyo State, Nigeria.
[5]Department of Physical Sciences, Chrisland University, P.M.B. 2131, Abeokuta, Ogun State, Nigeria
[6]Department of Agricultural Technology, Federal Polytechnic Ayede, Oyo State, Nigeria.
*Corresponding Author Email: isaac.olopade@fuwukari.edu.ng

ABSTRACT

In this research, a mathematical model is constructed to scrutinize the transmission patterns of monkeypox (mpox), with a specific emphasis on integrating the early detection of infected undetected individuals to curb its transmission. This research takes into account a range of factors influencing the propagation of monkeypox, encompassing population demographics, contact dynamics, and the efficacy of early detection of unidentified infected individuals. Employing the next-generation matrix method, the basic reproduction number(R_0) is computed, revealing that the disease-free equilibrium state is locally asymptotically stable when($R_0 < 1$). This suggests that containment of monkeypox is achievable within a human populace where (R_0) remains below one (1), yet it transitions to an endemic state when (R_0) exceeds this critical value one (1). Furthermore, a sensitivity analysis is conducted to evaluate the robustness of our findings to variations in model parameters. Utilizing numerical simulations conducted via MAPLE 18, we demonstrate the significance of prompt identification and immediate intervention for infected individuals who may otherwise go undetected, in effectively diminishing the dynamic propagation of monkeypox. The results underscore the pivotal role of early detection in mitigating monkeypox outbreaks and curtailing transmission rates.

Keywords:
Monkeypox,
Detection,
Equilibrium Points,
Stability,
Basic Reproduction Number.

INTRODUCTION

Orthopoxviruses present a significant global health concern, with Monkeypox (mpox) emerging as a prominent infectious disease (WHO, 2023). Initially identified in the Democratic Republic of the Congo around 1970 (Brown & Leggat, 2023; Jezek, 1988). Monkeypox has sporadically surfaced in West Africa (clade II) and Central and East Africa (clade I) (Brown & Leggat, 2023; Bunge et al., 2022). An outbreak in the United States in 2003 was attributed to the introduction of wild animals (clade II) (CDC, 2003; Larkin, 2003). Since 2005, the Democratic Republic of the Congo has consistently reported thousands of suspected cases annually (Hoff et al., 2017; WHO, 2023).

The Monkeypox outbreak initiated in Nigeria in 2017, with over 226 confirmed cases and 550 suspected cases reported by 2021(McCollum et al., 2023). Between 2018 and 2021, eight confirmed cases linked to travel from Nigeria were reported in other countries (McCollum et al., 2023). The monkeypoxvirus is classified into clade I and clade II, with clade I emerging in Sudanese locations for the first time (WHO, 2023). Symptoms typically include fever, swollen lymph nodes, and rash, but severe complications like encephalitis and myocarditis can occur (Alarcónn et al., 2023; Adler et al., 2022; Brown & Leggat, 2023; Mitjà et al., 2023; Markewitz et al., 2023; Nguyen et al., 2023). Notably, pregnancy-related infections can lead to miscarriage or stillbirth (WHO, 2022).

Smallpox vaccinations have shown efficacy in preventing Monkeypox cases, with newer vaccines offering enhanced safety (WHO, 2022). During outbreaks,

countries have administered third-generation smallpox vaccines like MVA-BN and LC16-KMB, previously unused in affected African nations (Priyamvada et al., 2022). Field research on these vaccines has been ongoing in the Democratic Republic of the Congo, where monkeypox cases have been steadily rising (Priyamvada et al., 2022).

Mathematical modeling has proven to be a valuable tool in understanding and predicting the dynamics of disease spread. Many researchers have utilized mathematical equations to model the transmission and progression of various diseases (Peter et al., 2020, Nguyen et al., 2021, Adesanya et al., 2016a; 2016b, Adewale et al., 2015a; 2015b; 2015c; 2016a; 2016b; Olopade et al., 2021a; 2021b;2017; 2016a; 2022, Akinwumi et al., 2021; Philemon et al., 2023. Adesola et al 2024a; 2024b, Ajao et al., 2023;Adeniran et al., 2023; Doty et al. 2017)

The exploration of pox-like dynamics associated with the monkeypox virus draws its foundation from the comprehensive study conducted by (Bhunu &Mushayabasa 2011). This seminal work serves as the bedrock for subsequent transmission analyses, providing invaluable insights into the intricate mechanisms underlying the spread of the virus. Building upon this groundwork, Bhunu et al.,(2009) presented compelling evidence showcasing the potential for disease eradication across both human and non-human primate populations through strategically planned treatment interventions. Their findings underscore the importance of proactive measures in controlling and ultimately eliminating the threat posed by the monkeypox virus.

(Usman & Adamu, 2017) study delves deeper into the dynamics of the monkeypox virus within both human hosts and rodent reservoirs. Through meticulous stability analyses, they elucidate the behavior of the virus within these populations, shedding light on critical factors influencing its transmission dynamics. In addition to these pivotal studies, researchers such as (Philemon et al., 2023;TeWinkel 2019; Somma et al. 2019; Bankuru et al., 2020; and Olumuyiwa et al. 2021). Each of these contributions adds a unique perspective to the broader discourse on monkeypox

The primary objective of this study is to develop a comprehensive mathematical model that integrates the detection of infected undetected infectious individuals into the dynamics of monkeypox transmission. By incorporating this crucial aspect into our model, we aim to delve deeper into understanding and quantifying the impact of detecting undetected infected individuals on the containment and mitigation of monkeypox spread.

In summary, the manuscript follows a structured approach, beginning with a detailed model formulation, followed by mathematical analysis, presentation of results and discussions and conclusions.

MATERIALS AND METHODS

Model Formulation

It is assumed that individuals contract the monkeypox infection through contact with infectious rodents, undetected infectious humans, and detected infectious humans at rates β_1, β_2 and β_3 respectively. Further details on parameters can be found in Table 2. The model is structured into two populations: human and rodent. The human population is further categorized into five compartments: i.e. S_h Susceptible human, E_h Exposed human, I_{hu} infected human undetected, I_{hd} infected human detected and R_h recovered human. The rodent population is divided into two compartments: S_r susceptible rodent and I_r Infected. Thus, we present seven nonlinear differential equations with mass action incidence rates as follows:

$$\begin{aligned}
\frac{dS_h}{dt} &= \pi_h - \lambda_h S_h - \mu_h S_h \\
\frac{dE_h}{dt} &= \lambda_h S_h - (\kappa_h + \mu_h) E_h \\
\frac{dI_{hu}}{dt} &= (1-\omega_h)\kappa_h E_h - (\tau_h + \mu_h + \delta_h) I_{hu} \\
\frac{dI_{hd}}{dt} &= \omega_h \kappa_h E_h + \tau_h I_{hu} - (\alpha_h + \mu_h + \delta_h) I_{hd} \\
\frac{dR_h}{dt} &= \alpha_h I_{hd} - \mu_h R_h \\
\frac{dS_r}{dt} &= \pi_r - \lambda_r S_r - \mu_r S_r \\
\frac{dI_r}{dt} &= \lambda_r S_r - \mu_r I_r
\end{aligned} \tag{1}$$

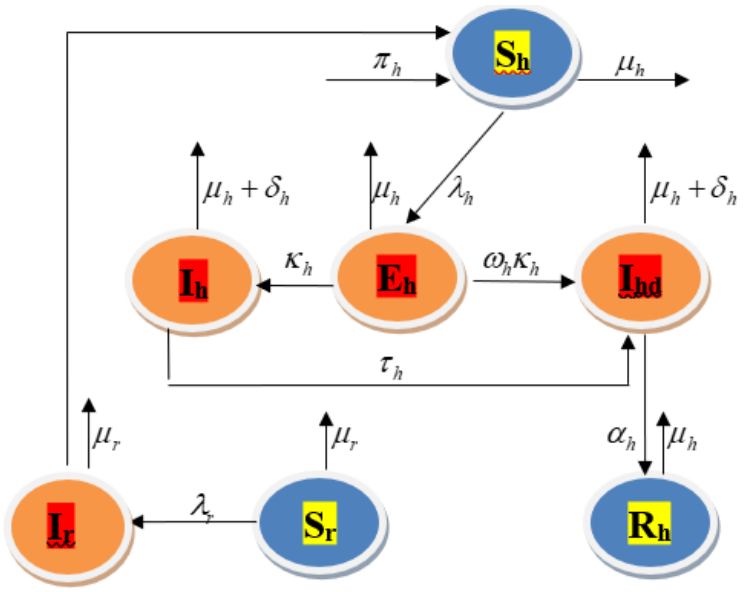

Figure 1: Schematic Diagram of the M-Pox Model.

Where the forces of infection induced by infectious rodent to susceptible human, infected undetected human to susceptible human, detected infectious human to susceptible human and infectious rodent to susceptible rodents are given below respectively;

$$\lambda_h = \frac{(\beta_1 I_r + \beta_2 I_{hu} + \beta_3 I_{hd})}{N_h}, \lambda_r = \frac{\beta_4 I_r}{N_r}$$

For better analysis;

$$\begin{aligned}
\frac{dS_h}{dt} &= \pi_h - \lambda_h S_h - \mu_h S_h \\
\frac{dE_h}{dt} &= \lambda_h S_h - K_1 E_h \\
\frac{dI_{hu}}{dt} &= (1-\omega_h)\kappa_h E_h - K_2 I_{hu} \\
\frac{dI_{hd}}{dt} &= \omega_h \kappa_h E_h + \tau_h I_{hu} - K_3 I_{hd} \\
\frac{dR_h}{dt} &= \alpha_h I_{hd} - \mu_h R_h \\
\frac{dS_r}{dt} &= \pi_r - \lambda_r S_r - \mu_r S_r \\
\frac{dI_r}{dt} &= \lambda_r S_r - \mu_r I_r
\end{aligned} \quad (2$$

Where$K_1 = (\kappa_h + \mu_h)$, $K_2 = (\tau_h + \mu_h + \delta_h)$,$K_3 = (\alpha_h + \mu_h + \delta_h)$

Table 1: Variable descriptions

VARIABLE	DESCRIPTIONS
S_h	Susceptible humans
E_h	Exposed humans
I_{hu}	Undetected Infected humans
I_{hd}	Undetected Infected humans
R_h	Recovered humans
S_r	Susceptible rodents
I_r	Infected rodents

Table 2: parameter values used for the simulations

Parameter	Value	Source	Description
π_h	0.029	Bhunu et al.(2009)	Recruitment rate for humans
π_r	0.2	Bhunu et al.(2009)	Recruitment rate for rodents
β_1	0.00025	Bhunu and mushayabasa (2011)	Rodent contact rate to Susceptible human
β_2	0.00006	Assumed	Undetected Infected Human to Susceptible human contact rate
β_3	0.00004	Bhunu and mushayabasa (2011)	Detected Infected Human to Susceptible human contact rate
β_4	0.027	Bhunu and mushayabasa (2011)	Rodent to Rodent Contact rate
α_h	2.0	Estimated	Recovery rate
τ_h	0.25	Assumed	Detection rate
μ_h	1.5	Bhunu and mushayabasa (2011)	Natural death of human
μ_r	0.002	Bhunu and mushayabasa (2011)	Natural death of rodents
δ_h	0.2	Assumed	Disease induced death rate for humans
κ_h	2.0	Estimated	Progression rate Fraction
ω_h	0.3	Assumed	of progression to infected detected

Table 3: Number of cumulative confirmed mpox cases and deaths reported to WHO, by WHO Region, from 1 January 2022 through 30 November 2023. Culled from WHO 2023

WHO Region	Total confirmed cases	Total Death	Cases in last Months	Monthly change in cases (%)
Region of the Americas	60 400	136	308	+110
European Region	26 654	7	259	+58
Western Pacific Region	2 760	3	172	-15
African Region	2126	22	58	-1.7
South-East Asia Region	748	2	109	-25.0
Eastern Mediterranean Region	95	1	0	-
Total	92 783	171	906	+25.7

Where the forces of infection induced by infectious rodent, infected undetected and detected infectious humans are given below respectively by $\lambda_h = \frac{(\beta_1 I_r + \beta_2 I_{hu} + \beta_3 I_{hd})}{N_h}, \lambda_r = \frac{\beta_4 I_r S_r}{N_h}$

The total human populations with respect to time are given by:

$$N_h(t) = S_h(t) + E_h(t) + I_{hu}(t) + I_{hd}(t) + R_h(t) \quad (3)$$

The total rodent populations with respect time are given by:

$$N_r(t) = S_r(t) + I_r(t) \quad (4)$$

All subject to the following nonnegative initial conditions:

$S_h(0) = S_h^0, E_h(0) = E_h^0, I_{hu}(0) = I_{hu}^0, I_{hd}(0) = I_{hd}^0, R_h(0) = R_h^0, S_r(0) = S_r^0, I_r(0) = I_r^0$

And $N(0) = N_0$

The derivative of (2) is given by:

$$\frac{dN_h}{dt} = \frac{dS_h}{dt} + \frac{dE_h}{dt} + \frac{dI_{hu}}{dt} + \frac{dI_{hd}}{dt} + \frac{dR_h}{dt} \quad (5)$$

Putting (1) into (5) gives

$$\frac{dN_h}{dt} = \pi_h - (I_{hu} + I_{hd})\delta - \mu_h N_h \quad (6)$$

Also, the derivative of (4) is given by

$$\frac{dN_r}{dt} = \frac{dS_r}{dt} + \frac{dI_r}{dt} \quad (7)$$

Putting (1) into (7) gives;

$$\frac{dN_r}{dt} = \pi_r - \mu_r N_r \quad (8)$$

Positivity of Solutions

For the model of Monkeypox to be epidemiologically meaningful and mathematically well posed, it is necessary to prove that all state variables are non-negative for all $t > 0$.

Theorem 1

Let:

$$S_h(0) \geq 0, E_h(0) \geq 0, I_{hu}(0) \geq 0, I_{hd}(0) \geq 0, R_h(0) \geq 0, S_r(0) \geq 0, I_r(0) \geq 0\} \in \Gamma \quad (9)$$

Then, the solution:

$\{S_h(t), E_h(t), I_{hu}(t), I_{hd}(t), R_h(t), S_r(t), I_r(t)\}$ of the model system equation (1) are positive $\forall t \geq 0$.

Proof:

$$\frac{dN_h}{dt} \leq \pi_h - \mu_h N_h \quad (10)$$

Since $(I_{hu} = I_{hd} = 0)$

Rearrangement of (10), gives;

$$\frac{dN_h}{dt} + \mu_h N_h \leq \pi_h \quad (11)$$

From which it follows that:

I.F.=$\ell^{\int \mu_h dt} = \ell^{\mu_h t}$

Multiplying (11) by the Integrating factor on both sides will give:

$$\ell^{\mu_h t}\frac{dN_h}{dt} + \mu_h N_h \ell^{\mu_h t} \leq \pi_h \ell^{\mu_h t} \quad (12)$$

It then follows that:

$$\frac{d}{dt}(\mu_h N_h \ell^{\mu_h t}) \leq \pi_h \ell^{\mu_h t}$$

Integrating on both sides gives:

$N_h(t)\ell^{\mu_h t} \leq \frac{\pi_h}{\mu_h}\ell^{\mu_h t} + C$Where C is a constant of the integration, it follows that:

$$N_h(t) \leq \frac{\pi_h}{\mu_h} + C\ell^{-\mu_h t} \quad (13)$$

Applying the initial condition that, when $t = 0, N_h(0) = N_h^0$, we have:

$$N_h^0 - \frac{\pi_h}{\mu_h} \leq C \quad (14)$$

Putting (14) into (13), gives;

$$N_h(t) \leq \frac{\pi_h}{\mu_h} + \left(N_h^0 - \frac{\pi_h}{\mu_h}\right)\ell^{-\mu_h t} \quad (15)$$

$0 \leq N_h(t) \leq \frac{\pi_h}{\mu_h}ast \to \infty$

Therefore, Monkeypox model formulated is mathematically and epidemiologically well posed.

Stability of the Disease Free Equilibrium (DFE)

Disease-free equilibrium

For critical points, we set:

$$\frac{dS_h}{dt} = \frac{dE_h}{dt} = \frac{dI_{hu}}{dt} = \frac{dI_{hd}}{dt} = \frac{dR_h}{dt} = \frac{dS_r}{dt} = \frac{dI_r}{dt} = 0 \quad (16)$$

At this free equilibrium, it is assumed that there is no infection, and then we set

So $E_h = I_{hu} = I_{hd} = R_h = I_r = 0$

$$\varepsilon_0 = (S_h, E_h, I_{hu}, I_{hd}, \rightleftarrows R_h, S_r, I_r) = \left(\frac{\pi_h}{\mu_h}, 0,0,0,0, \frac{\pi_r}{\mu_r}, 0\right)$$

Disease free equilibrium is:

$$\varepsilon_0 = \left(\frac{\pi_h}{\mu_h}, 0,0,0,0, \frac{\theta_r}{\mu_r}, 0\right)$$

Endemic equilibrium

Let $\varepsilon_1 = (S_h{}^*, E_h{}^*, I_{hu}{}^*, I_{hd}{}^*, R_h{}^*, S_r^*, I_r^*)$ represents any arbitrary endemic equilibrium of the model equation. Solving the equations of the system at the steady-state goes thus:

$$S_h^* = \frac{\pi_h}{\lambda^*{}_h + \mu_h} \tag{17}$$

$$E_h^* = \frac{\lambda^*{}_h S_h^*}{K_1} = \frac{\pi_h \lambda^*{}_h}{(\lambda^*{}_h + \mu_h)K_1} \tag{18}$$

$$I_{hu}^* = \frac{(1-\omega_h)\kappa_h E_h^*}{K_2} = \frac{\pi_h \lambda^*{}_h}{(\lambda^*{}_h + \mu_h)K_1}\left\{\frac{(1-\omega_h)\kappa_h}{K_2}\right\} = \frac{(1-\omega_h)\kappa_h \lambda_h^* \pi_h}{K_1 K_2 (\lambda^*{}_h + \mu_h)} \tag{19}$$

$$I_{hd}^* = \frac{\omega_h \kappa_h E^*{}_h + \tau_h I_{hu}^*}{K_3} = \frac{\pi_h \lambda^*{}_h \omega_h \kappa_h}{(\lambda^*{}_h + \mu_h)K_1 K_3} + \frac{(1-\omega_h)\kappa_h \pi_h \lambda^*{}_h \tau_h}{(\lambda^*{}_h + \mu_h)K_1 K_3 K_2}$$

$$= \frac{\pi_h \lambda^*{}_h \omega_h \kappa_h K_2 + \kappa_h \pi_h \lambda^*{}_h \tau_h - \omega_h \kappa_h \pi_h \lambda^*{}_h \tau_h}{(\lambda^*{}_h + \mu_h)K_1 K_2 K_3}$$

.

$$= \frac{\lambda^*{}_h \kappa_h \pi_h (\tau_h + \mu_h \omega_h + \omega_h \delta_h)}{(\lambda^*{}_h + \mu_h)K_1 K_2 K_3} \tag{20}$$

$$R_h^* = \frac{\alpha_h I_{hd}^*}{\mu_h} = \frac{\lambda^*{}_h \kappa_h \pi_h \alpha_h (\tau_h + \mu_h \omega_h + \omega_h \delta_h)}{(\lambda^*{}_h + \mu_h)\mu_h K_1 K_2 K_3} \tag{21}$$

$$S_r^* = \frac{\pi_r}{\lambda^*{}_r + \mu_r} \tag{22}$$

$$I_r^* = \frac{\lambda^*{}_r S_r^*}{\mu_r} = \frac{\pi_r \lambda^*{}_r}{(\lambda^*{}_r + \mu_r)\mu_r} \tag{23}$$

The endemic equilibrium points are equations (17)-(23) above.

Basic Reproduction Number

The basic reproduction number of the model (1) is calculated by using the next generation matrix (Olopade et al., 2022; 2024; Akinola et al., 2021). Using this approach, we have:

$$Fi = \begin{pmatrix} F1 \\ F2 \\ F3 \\ F4 \end{pmatrix} = \begin{pmatrix} \lambda_h S_h \\ 0 \\ 0 \\ \lambda_r S_r \end{pmatrix} \tag{24}$$

$$Vi = \begin{pmatrix} V1 \\ V2 \\ V3 \\ V4 \end{pmatrix} = \begin{pmatrix} -(\kappa_h + \mu_h)E_h \\ (1-\omega_h)\kappa_h E_h - (\tau_h + \mu_h + \delta_h)I_{hu} \\ \omega_h \kappa_h E_h + \tau_h I_{hu} - (\alpha_h + \mu_h + \delta_h)I_{hd} \\ -\mu_r I_r \end{pmatrix} \tag{25}$$

After taking partial derivatives F and V, we have:

$$F = \begin{pmatrix} 0 & \beta_2 & \beta_3 & \beta_1 \\ 0 & 0 & 0 & 0 \\ 0 & 0 & 0 & 0 \\ 0 & 0 & 0 & \beta_4 \end{pmatrix} \tag{26}$$

$$V = \begin{pmatrix} K_1 & 0 & 0 & 0 \\ -(1-\omega_h)\kappa_h & K_2 & 0 & 0 \\ -\omega_h \kappa_h & -\tau_h & K_3 & 0 \\ 0 & 0 & 0 & \mu_r \end{pmatrix} \tag{27}$$

The reproduction number is the dominant eigen-value of$F \times V^{-1}$. Thus,

$$R_{MP} = \frac{(((K_2 - \tau_h)\beta_3 - \beta_2 K_3)\omega_h + \beta_2 K_3 + \beta_3 \tau_h)\tau_h}{K_3 K_2 K_1} \tag{28}$$

Local Stability of Disease-Free Equilibrium (DFE)

Theorem 2: The disease-free equilibrium of the system (2) is locally asymptotically stable (LAS) if $R_0 < 1$ and unstable if$R_0 > 1$.

Proof: Thus, the theorem implies that the disease can be eliminated from the community. Now to determine the local stability of E_0, the following Jacobian matrix is computed corresponding to equilibrium point E_0. Considering the stability of the disease-free equilibrium at the critical point (0,0,0,0,0,0,0) of equation (2), we have:

$$J_{MP} = \begin{pmatrix} -\mu & 0 & 0 & 0 & 0 & 0 & 0 \\ 0 & -K_1 & 0 & 0 & 0 & 0 & 0 \\ 0 & (1-\omega_h)\kappa_h & -K_2 & 0 & 0 & 0 & 0 \\ 0 & \omega_h\kappa_h & \tau_h & -K_3 & 0 & 0 & 0 \\ 0 & 0 & 0 & \alpha_h & -\mu_h & 0 & 0 \\ 0 & 0 & 0 & 0 & 0 & -\mu_r & 0 \\ 0 & 0 & 0 & 0 & 0 & 0 & -\mu_r \end{pmatrix} \quad (29)$$

Then the characteristic equations are obtained as, $|J_{MP} - \lambda I| = 0$ (where I is 7*7 identity matrix).

Where:

$$\lambda I = \begin{bmatrix} \lambda & 0 & 0 & 0 & 0 & 0 & 0 \\ 0 & \lambda & 0 & 0 & 0 & 0 & 0 \\ 0 & 0 & \lambda & 0 & 0 & 0 & 0 \\ 0 & 0 & 0 & \lambda & 0 & 0 & 0 \\ 0 & 0 & 0 & 0 & \lambda & 0 & 0 \\ 0 & 0 & 0 & 0 & 0 & \lambda & 0 \\ 0 & 0 & 0 & 0 & 0 & 0 & \lambda \end{bmatrix} \quad (30)$$

Hence,$|J_{MP} - \lambda I| = 0$ implies that

Hence, the corresponding eigenvalues of equation are:

$\lambda_1 = -\mu, \lambda_2 = -K_1, \lambda_3 = -K_2, \lambda_4 = -K_3, \lambda_5 = -\mu_h, \lambda_6 = -\mu_r,$ and$\lambda_7 = -\mu_r$

Since all the real roots are negative, real and distinct. Hence, disease-free equilibrium of the model (2) is locally asymptotically stable (LAS).

Global Asymptotic Stability of the Disease-Free Equilibrium (GASDFE)

We adopt the method used by Castillo-Chavez & Song. (2004) for the investigation of the global asymptotic stability of the disease free equilibrium of the model. The two conditions stated in the method presented by Castillo-Chavez & Song. (2004) must be met for the disease free equilibrium to be globally asymptotically stable.

The system of the equations of the equations of the model (2) can be written in the form

$$\frac{dM}{dt} = F(M, I) \quad (31)$$

and

$$\frac{dM}{dt} = G(M, I) \quad (32)$$

With$G(M, 0) = 0$, where $M \in R^3$represents the uninfected classes $(S_h, \rightleftarrows R_h, \rightleftarrows S_r)$ and $I \in R^4$ represents the infected classes $(E_h, \rightleftarrows \rightleftarrows \rightleftarrows I_{hu}, \rightleftarrows I_{hd}, \rightleftarrows I_r)$

Also, $E_0 = F(M^*, 0)$ denotes the disease free equilibrium of the model.

Then, the two conditions $(H1)$ and $(H2)$ below must be satisfied for the model to be globally asymptotically stable;

$$(H1): \quad \frac{dM}{dt} = F(M,0), M^* \text{Globally asymptotically stable}$$

$(H2): G(M, I) = BI - \hat{G}(M, I), \hat{G}(M, I) \geq 0for(M, I) \in \Omega$. Where $B = D, G(M^*, 0)$ is an M-matrix (The off diagonal elements of B are non-negative) and $\Omega$is the region where the model is biologically meaningful. If $(H1)$ and $(H2)$ are satisfied, then the following theorem holds.

Theorem 3; The disease free equilibrium $E_0 = (M^*, 0)$ is globally asymptotically stable if $R_0 \prec 1$and that the condition $(H1)$ and $(H2)$ are satisfied.

Proof: Note that $M = (S_h, \rightleftarrows R_h, \rightleftarrows S_r)$ and $I = (E_h, \rightleftarrows \rightleftarrows \rightleftarrows I_{ha}, \rightleftarrows I_{hs}, \rightleftarrows R_h, \rightleftarrows I_r)$

$$F(M,0)=\begin{pmatrix}\pi_h-\mu_h S_h\\0\\0\end{pmatrix} \quad (33)$$

an

$$B=\begin{pmatrix}-K_1 & \beta_2 & \beta_3 & \beta_1\\(1-\omega_h)\kappa_h & -K_2 & 0 & 0\\\omega_h\kappa_h & \tau_h & -K_3 & 0\\0 & 0 & 0 & \beta_4\end{pmatrix} \quad (34)$$

$$\hat{G}(M,I)=\begin{bmatrix}[\beta_1 I_r+\beta_2 I_{hd}+\beta_3 I_{hs}]\left(1-\frac{S_h}{N_h}\right)\\0\\0\\\beta_4 I_r\left(1-\frac{S_r}{N_r}\right)\end{bmatrix} \quad (35)$$

Since$0\le S_h\le N_h$ and $0\le S_r\le N_r$it is clearly seen that $\hat{G}(M,I)$ Also, $M^*=\left(\frac{\pi}{\mu_h},0\right)$is globally asymptotically stable equilibrium of $\frac{dM}{dt}=F(M,0)$. Therefore, the disease free equilibrium is globally asymptotically stable when $R_0<1$.

Theorem 4: Let $\varepsilon*$ be the unique positive equilibrium point of the system (1), If$R_0>1$, then endemic equilibrium $\varepsilon*$ of the system (1) is globally asymptotically stable.
Proof: Using theorem 5 and 6, consider;

Theorem 5: (Dulac's Criterion)
Consider the following general nonlinear autonomous system
$x(t)=f(x),x\in E$ (36)
Let $f=C^I(E)$ where E is a simple connected region inR^n. If there exists a function $H\in C^I(E)$ such that $\nabla.(H.f)$ is not identically zero and does not change sign in E, the system (36) has no close orbit lying entirely in E. if A is anannular region contained in E on which $\nabla.(H.f)$ does not change sign, then there is at most one limit cycle of thesystem (36) in A.

Theorem 6: (The Poincare-Bendixson Theorem): Suppose that $f\in C^I(E)$
Where E is an open subset of $R^n$and that the system (36) has a trajectory Γ contained in a compact subset $f$of E. Assume that the system (36) has only one unique equilibrium point $x_0$in f, then one of the following possibilities holds.
(1) $w(\Gamma)$ is the equilibrium point x
(2) $w(\Gamma)$ is a periodic orbit
(3) $w(\Gamma)$ is a graphic
$H(S_h,E_h,I_{hu},I_{hd},R_h,S_r,I_r)=\frac{1}{S_hE_hI_{hu}I_{hd}R_hS_rI_r},S_h>0,E_h>0,I_{hu}>0,I_{hd}>0,R_h>0,S_r>0,$ and$I_r>0,$
Then,

$$\nabla.(H.f)=\frac{\partial}{\partial S_h}(H.f_1)+\frac{\partial}{\partial E_h}(H.f_2)+\frac{\partial}{\partial I_{hu}}(H.f_3)\frac{\partial}{\partial I_{hd}}+(H.f_4)+\frac{\partial}{\partial R_h}(H.f_5)+\frac{\partial}{\partial S_r}(H.f_6)+\frac{\partial}{\partial I_r}(H.f_6) \quad (37)$$

$$\frac{\partial}{\partial S_h}\left[\frac{1}{S_hE_hI_{hu}I_{hd}R_hS_rI_r}(\pi_h-\lambda_hS_h-\mu_hS_h)\right]+\frac{\partial}{\partial E_h}\left[\frac{1}{S_hE_hI_{hu}I_{hd}R_hS_rI_r}(\lambda_hS_h-(\kappa_h+\mu_h)E_h)\right]$$
$$+\frac{\partial}{\partial I_{hu}}\left[\frac{1}{S_hE_hI_{hu}I_{hd}R_hS_rI_r}\begin{pmatrix}(1-\omega_h)\kappa_hE_h\\-(\tau_h+\mu_h+\delta_h)I_{hu}\end{pmatrix}\right]+\frac{\partial}{\partial I_{hd}}\left[\frac{1}{S_hE_hI_{hu}I_{hd}R_hS_rI_r}\begin{pmatrix}\omega_h\kappa_hE_h+\tau_hI_{hu}\\-(\alpha_h+\mu_h+\delta_h)I_{hd}\end{pmatrix}\right]$$
$$+\frac{\partial}{\partial R_h}\left[\frac{1}{S_hE_hI_{hu}I_{hd}R_hS_rI_r}(\alpha_hI_{hd}-\mu_hR_h)\right]+\frac{\partial}{\partial S_r}\left[\frac{1}{S_hE_hI_{hu}I_{hd}R_hS_rI_r}(\pi_r-\lambda_rS_r-\mu_rS_r)\right]$$
$$+\frac{\partial}{\partial I_r}\left[\frac{1}{S_hE_hI_{hu}I_{hd}R_hS_rI_r}(\lambda_rS_r-\mu_rI_r)\right]$$

$$= -\frac{\pi_h}{(S_h)^2 E_h I_{hu} I_{hd} R_h S_r I_r} - \frac{\lambda_h}{(E_h)^2 I_{hu} I_{hd} R_h S_r I_r} - \frac{(1-\omega_h)\kappa_h}{S_h (I_{hu})^2 I_{hd} R_h S_r I_r} - \frac{\omega_h \kappa_h}{S_h I_{hu} (I_{hd})^2 R_h S_r I_r}$$
$$- \frac{\tau_h}{S_h E_h (I_{hd})^2 R_h S_r I_r} - \frac{\alpha_h}{S_h E_h I_{hu} (R_h)^2 S_r I_r} - \frac{\pi_r}{S_h E_h I_{hu} I_{hd} R_h (S_r)^2 I_r} - \frac{\lambda_r}{S_h E_h I_{hu} I_{hd} R_h (I_r)^2}$$

(38)

$$= -\left[\begin{array}{l} \frac{\pi_h}{(S_h)^2 E_h I_{hu} I_{hd} R_h S_r I_r} + \frac{\lambda_h}{(E_h)^2 I_{hu} I_{hd} R_h S_r I_r} + \frac{(1-\omega_h)\kappa_h}{S_h (I_{hu})^2 I_{hd} R_h S_r I_r} \\ + \frac{\omega_h \kappa_h}{S_h I_{hu} (I_{hd})^2 R_h S_r I_r} + \frac{\tau_h}{S_h E_h (I_{hd})^2 R_h S_r I_r} + \frac{\alpha_h}{S_h E_h I_{hu} (R_h)^2 S_r I_r} \\ + \frac{\pi_r}{S_h E_h I_{hu} I_{hd} R_h (S_r)^2 I_r} + \frac{\lambda_r}{S_h E_h I_{hu} I_{hd} R_h (I_r)^2} \end{array}\right] < 0 \quad (39)$$

Consequently, as per Dulac's criterion, a closed orbit exists in the first quadrant, implying that the endemic equilibrium is globally asymptotically stable.

Sensitivity Analysis

Since the basic reproduction number (R_0) is crucial for predicting disease progression, a sensitivity analysis is conducted to ascertain which model parameters predominantly influence(R_0). The sensitivity index is calculated using the following formula,

$$X_P^{R_0} = \frac{d\omega}{dP} \times \frac{P}{R_0} \quad (40)$$

A negative sensitivity index indicates an inverse relationship between the parameter and(R_0). Conversely, a positive sensitivity index suggests that (R_0) increases as the relevant parameter rises. The sensitivity index of (R_0) with respect to each parameter is calculated using the data in Table 2. The estimated sensitivity indices for (R_0) are presented in Table 4. From Table 4, it is evident that an increase in the values of parameters such as alpha, beta, gamma, delta, and epsilon results in a decrease in the value of (R_0) i. Conversely, an increase in the values of parameters theta and mu leads to an increase in monkeypox cases.

Table 4: Sensitivity Index of Parameters

Parameter	SensitivityValue	Sign
β_2	1.000000	+
β_3	1.000000	+
α_h	-0.575446	-
τ_h	-0.875647	-
μ_h	-0.678791	-
δ_h	-0.543674	-
κ_h	0.736363	+
ω_h	0.613456	+

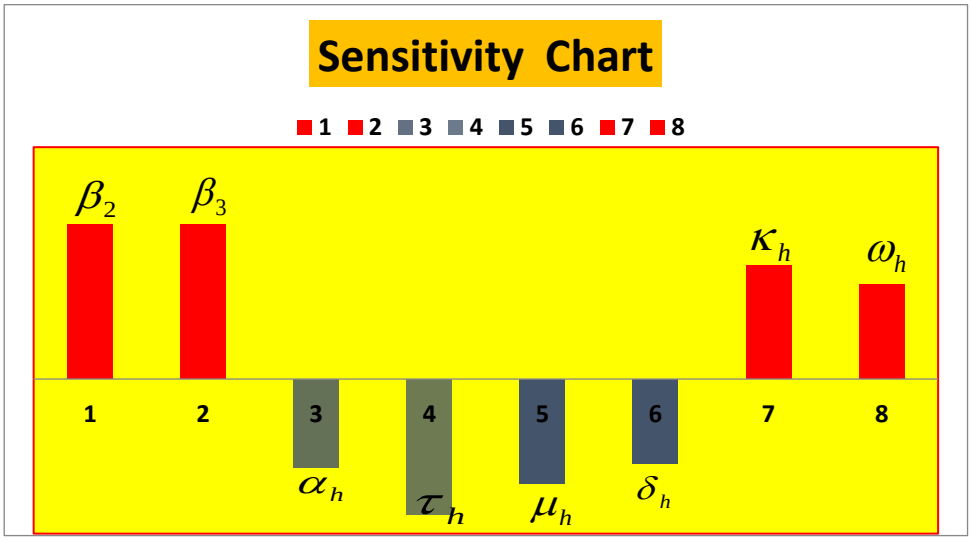

Figure 2: Sensitivity Chart of Monkeypox Model

Numerical Simulation

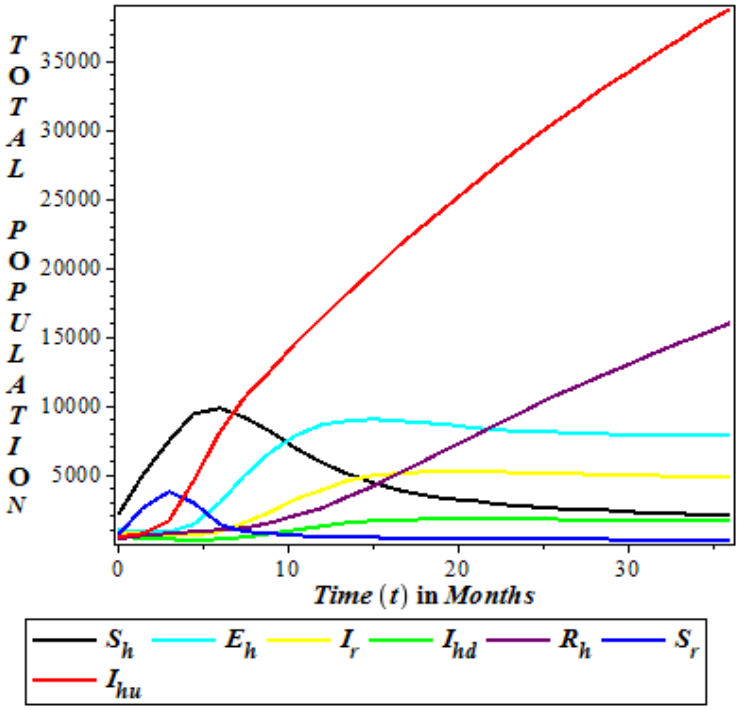

Figure 3: The total population of $S_h, E_h, I_{hu}, I_{hd}, R_h, S_r$&$I_r$ when $\tau_h = 0.0$

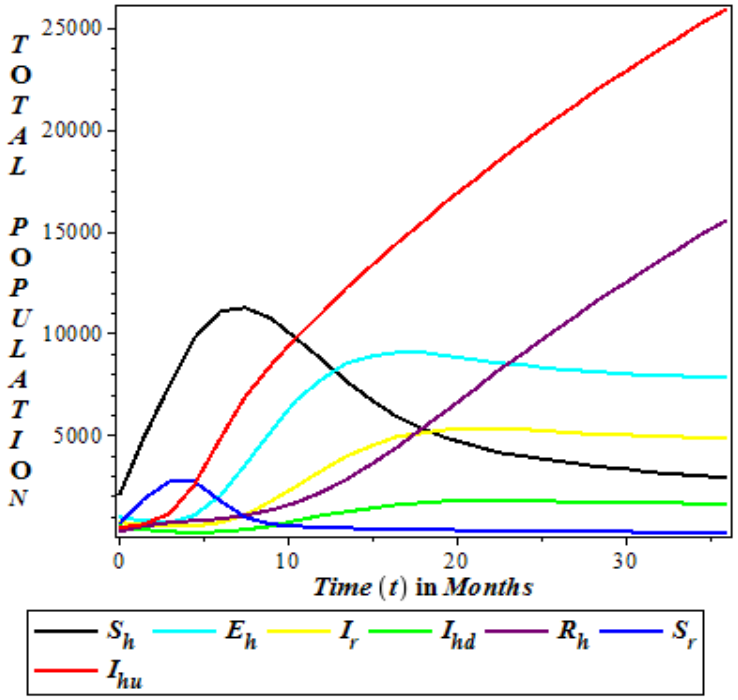

Figure 4: The total population of $S_h, E_h, I_{hu}, I_{hd}, R_h, S_r$ & I_r when $\tau_h = 0.25$

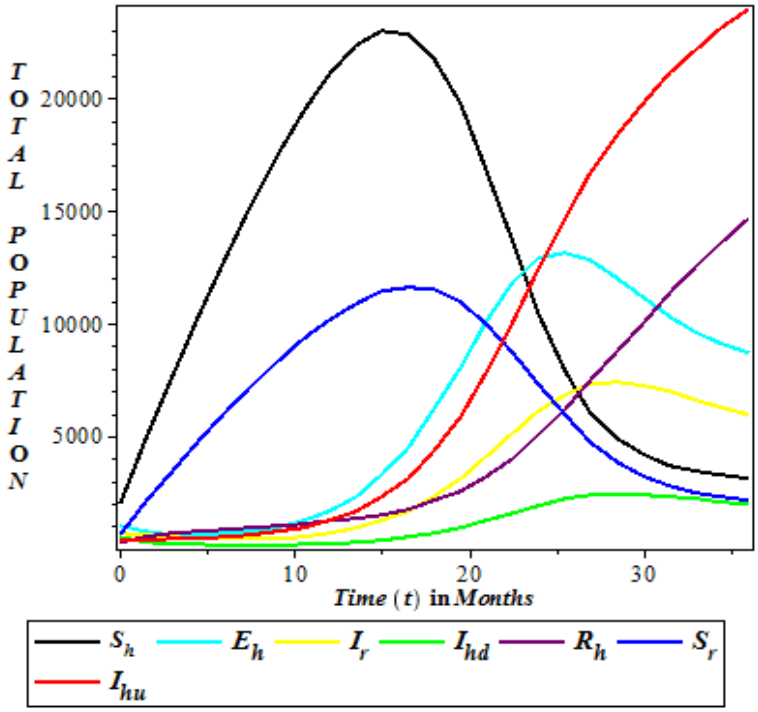

Figure 5: The total population of $S_h, E_h, I_{hu}, I_{hd}, R_h, S_r$ & I_r when $\tau_h = 0.4$

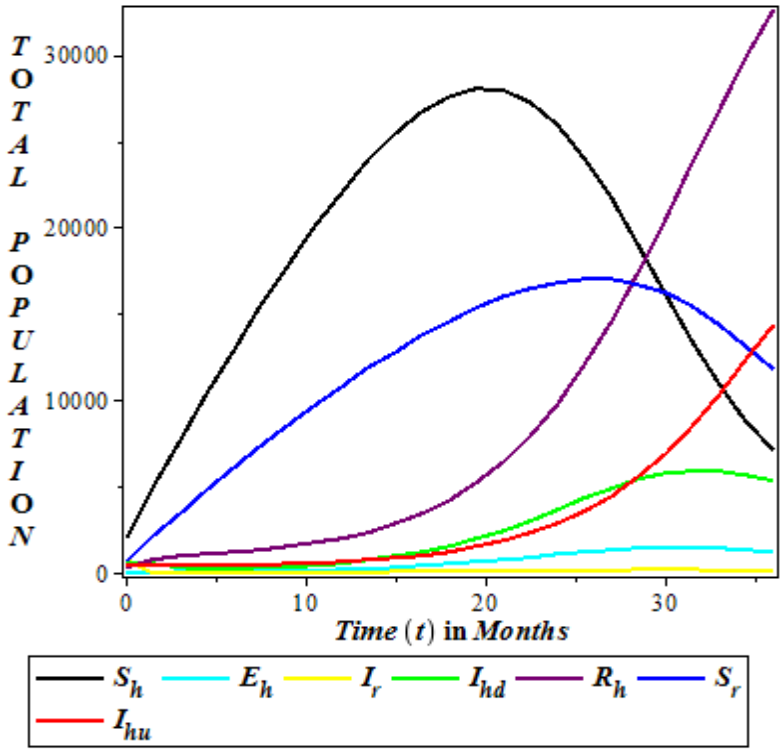

Figure 6: The total population of $S_h, E_h, I_{hu}, I_{hd}, R_h, S_r$ & I_r when $\tau_h = 0.7$

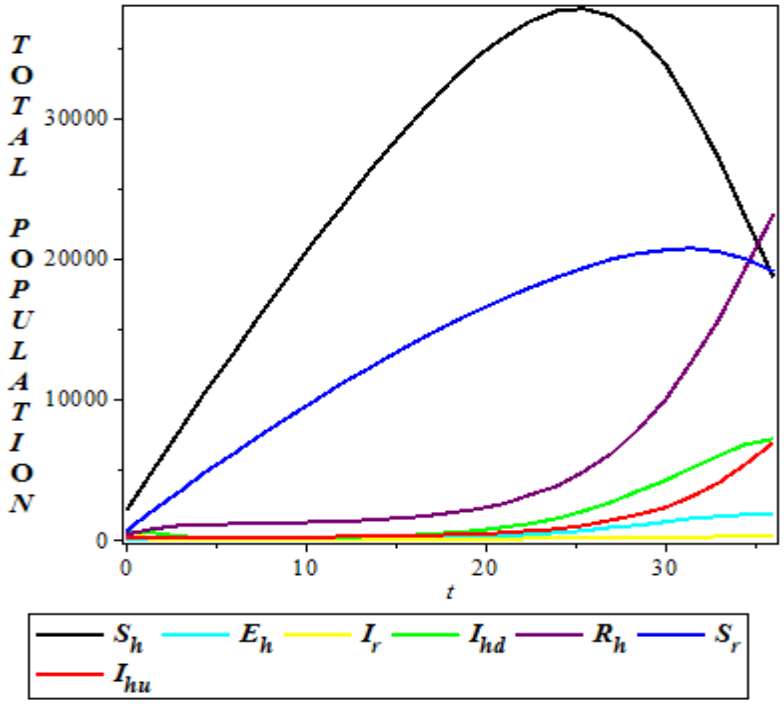

Figure 7: The total population of $S_h, E_h, I_{hu}, I_{hd}, R_h, S_r$ & I_r when $\tau_h = 1$

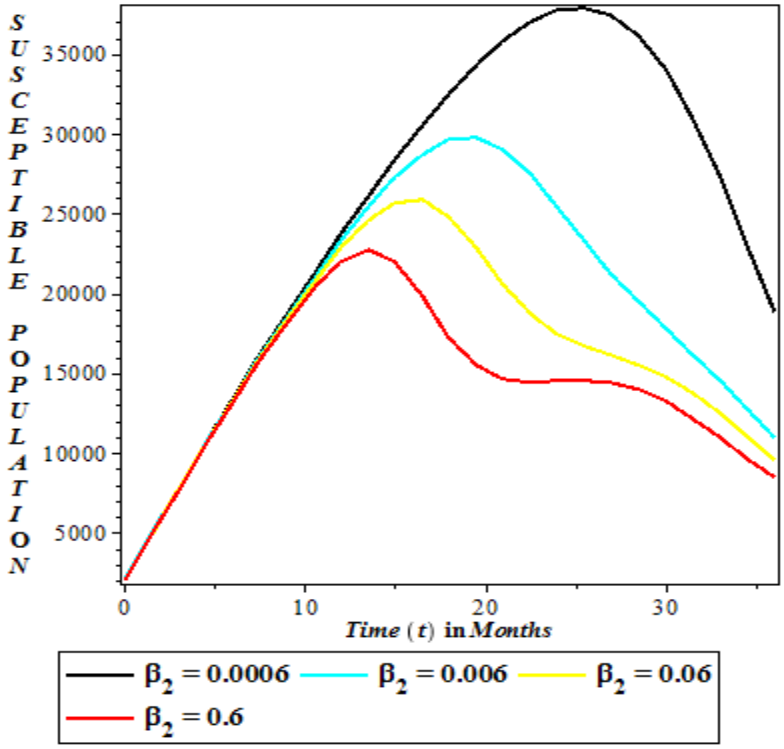

Figure 8: The Susceptible population with different values of β_2

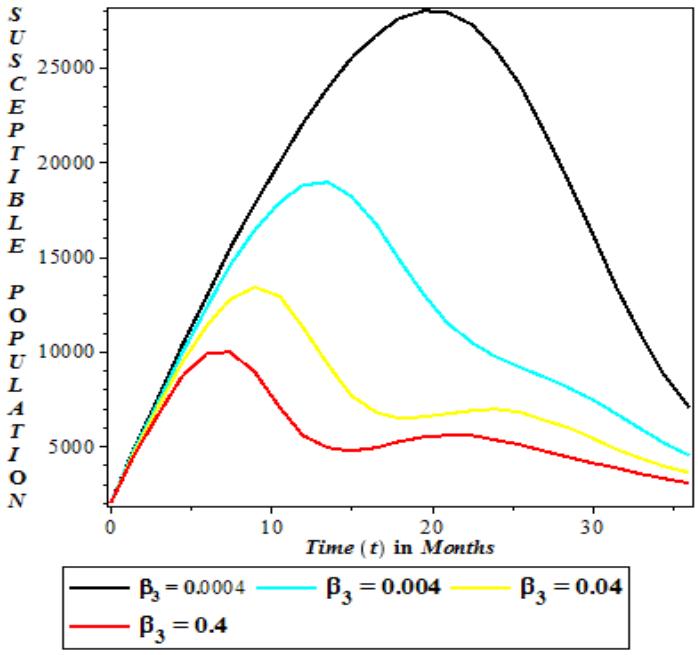

Figure 9: The Susceptible population with different values of β_3

RESULTS AND DISCUSSION

We present and thoroughly analyze a deterministic model consisting of seven nonlinear differential equations for monkeypox, incorporating the detection of undetected infected humans. The positivity of the solution demonstrates that the model is both mathematically and epidemiologically well-defined. We examine the existence of disease-free and endemic equilibrium points, with the basic reproduction number (R0) serving as a crucial determinant of the disease's dynamics. Specifically, R0, representing the average number of new secondary infections generated by a single infected human during their infectious period, dictates whether monkeypox will diminish (i.e., when R0 < 1) or proliferate (i.e., when R0 > 1). We delve into the global stability analysis of both disease-free and endemic equilibria. Furthermore, we conduct numerical simulations for sensitivity analysis using MAPLE 18 software. This allows us to identify the parameters that significantly influence the spread of monkeypox among humans and assess how early detection measures could serve as effective control strategies to prevent the endemic transmission of monkeypox within human populations.

From January 1, 2022, to November 30, 2023, the World Health Organization (WHO) received reports of 92,783 laboratory-confirmed cases of mpox, accompanied by 171 deaths, spanning across 116 countries/territories/areas globally. These cases were distributed across all six WHO Regions, as outlined in Table 3. During November 2023, an additional 906 new cases were reported, indicating a notable 26% increase compared to the preceding month. Notably, the majority of these cases were concentrated in the Region of the Americas (34%) and the European Region (29%). This surge underscores the ongoing challenge posed by Mpox and highlights the importance of continued surveillance and response efforts across affected regions to mitigate its impact on public health.The data underscores the urgency for coordinated international action to combat the spread of mpox and underscores the need for enhanced surveillance, prevention, and control measures to curb its transmission and minimize its adverse effects on global health.

Figures 3-7 serve as indispensable tools for understanding the pivotal role of the detection rate in shaping the dynamics of mpox disease outbreaks. These graphs offer a nuanced exploration of the intricate relationship between detection efforts and the prevalence of infected but undetected individuals within a population. While the concept of detection rate may appear straightforward at first glance, these figures unveil the multifaceted impact it has on the trajectory of Mpox outbreaks and the effectiveness of interventions designed to mitigate its spread.Indeed, the implications of these findings extend far beyond mere statistical correlations. They underscore the indispensable role of timely detection in disrupting chains of transmission and curtailing the spread of mpox within communities. Through meticulous analysis of the data presented in these figures, we gain a deeper appreciation for the profound impact that detection efforts can have on the course of mpox outbreaks and the overall effectiveness of public health interventions.

The relationship between the detection rate and the prevalence of infectious persons who have not yet been detected in cases of monkeypox is depicted in Figure 3. It draws attention to a worrying pattern in which the prevalence of cases that go undiagnosed rises dramatically when the detection rate drops to zero (0). The graph shows a rapid increase in the population's number of infected persons who are not yet detected as infectious when the detection rate is zero (0). This situation highlights the dire repercussions of weak or nonexistent detection attempts. The virus can spread quickly across the population in the absence of effective methods for detecting and isolating affected people, creating a huge pool of undiagnosed cases.Figure 4 demonstrates the impact of a detection rate of 0.25 on reducing the prevalence of infected undetected infectious individuals in mpox disease dynamics. Initially, the graph shows a high prevalence of undetected infected individuals, with a count of 39,000. However, as the detection rate improves to 0.25, there is a noticeable decline in this number over time, gradually reducing to 26,000. This reduction underscores the effectiveness of enhanced detection efforts in identifying and curtails mpox cases, thus curbing further transmission and mitigating the spread of the disease.

The effect of a detection rate of 0.4 on reducing the proportion of infectious persons who are infected but have not been detected is seen in Figure 5 for the dynamics of the mpox illness. First, the graph shows a significant number of undiagnosed sick people, which is 26,000 in total. This number does, however, show a noticeable downward trend over time as the detection rate improves to 0.4, eventually falling to 24,000. This decline is evidence of how well increased detection measures have worked to identify mpox cases.In Figure 6, we witness how elevating the detection rate to 0.7 influences the decline in the prevalence of undetected infected individuals in mpox disease dynamics. At the outset, the graph reveals a population of 24,000 undetected infected cases. Yet, with the advancement of the detection rate, this figure steadily diminishes over time, reaching 13,000. This downward trend emphasizes the efficacy of bolstered detection measures in pinpointing and isolating mpox cases, consequently curtailing further transmission and containing the disease's spread.

Figure 7 demonstrates the significant impact of increasing the detection rate to 1 on reducing the prevalence of undetected infected individuals in mpox disease dynamics. Initially, the graph depicts a population of 13,000 undetected infected cases. However, as the detection rate rises, this number steadily decreases over time, ultimately reaching 6,000. This decline underscores the effectiveness of improved detection measures in identifying and treating mpox cases, thereby limiting further transmission and containing the spread of the disease. Overall, Figure 7 underscores the crucial role of enhanced detection rates in managing mpox outbreaks and protecting public health. Figure 8 illustrates the impact of the effective contact rate of undetected infected individuals with mpox on the susceptible population. The results indicate that as the effective contact rate increases, there is a corresponding decrease in the susceptible population. This trend suggests that higher levels of effective contact between undetected infected individuals and the susceptible population lead to a more rapid spread of mpox, resulting in a reduction of individuals who remain susceptible to the disease. The influence of the effective contact rate of individuals with mpox who have been detected infected on the vulnerable population is illustrated in Figure 9. The vulnerable population declines proportionately with an increase in the effective contact rate. This implies that more interaction between the susceptible population and those who have been found to be sick speeds up the spread of mpox, hence decreasing the number of susceptible people. The figure highlights the necessity of controlling effective contact rates in order to prevent the spread of mpox and safeguard the vulnerable population.

CONCLUSION

Conclusively, the significance of the detection rate in mpox disease dynamics underscores the pivotal role of surveillance, early detection, and containment measures in controlling outbreaks. Efforts to enhance case detection, reporting, and data collection are imperative for gaining a comprehensive understanding of the disease burden and implementing targeted interventions to mitigate its impact on public health

REFERENCES

Alarcón J., Kim M., Terashita D., Davar K., Garrigues J. M., &Guccione J. P.(2023). An Mpox-Related Death in the United States. *N Engl J Med*, 388(13): 1246–1257.

Adesanya A. O., Olopade I. A., Akanni J. O., Oladapo A. O. &Omoloye M. A.(2016b).Mathematical and Sensitivity Analysis of Efficacy of Condom on the Dynamical Transmission of Gonorrhoea Disease. *Imperial Journal of Interdisciplinary Research (IJIR)***.** 2(11): 368-375.

Adesanya A.O., Olopade I. A., Akinwumi T. O. & Adesanya A. A. (2016). Mathematical Analysis of Early Treatment of Gonorrhea Infection. *American International Journal of Research in Science, Technology, Engineering & Mathematics,* 15(2).

Adesola O. I., Oloruntoyin S. S., Emmanuel P. M., Temilade M. I., Adeyemi A. G., Oladele A. S., Mamman A. U., & Kareem A. A. (2024). Mathematical Modelling and Analyzing the Dynamics of Condom Efficacy and

Compliance in the Spread of HIV/AIDS. *Asian Research Journal of Current Science*. 6(1): 54–65.

Adesola O. I., Temilade M. I., Emmanuel P. M., Oladele A. S., Adeyemi A. G., Sunday S. & Olumuyiwa A. S. (2024). Mathematical Analysis of Optimal Control of Human Immunodeficiency Virus (HIV) Co-infection with Tuberculosis (TB). *Asian Research Journal of Current Science*, 6(1): 23–53.

Adewale, S. O, Olopade, I. A., Adeniran, G. A., Mohammed, I. T. and Ajao, S. O. (2015a). Mathematical Analysis of Effects of Isolation On Ebola Transmission Dynamics. *Researchjournali's Journal of Mathematics*. Vol. 2, No. 2. Pp. 1-20.

Adewale S. O., Olopade I. A., Adeniran G. A., Mohammed I. T., & Ajao S. O. (2015b). Mathematical Analysis of Effects of Isolation on Ebola Transmission Dynamics. *Researchjournali's Journal of Mathematics*. 2(2):1-20.

Adewale S. O., Olopade I. A., & Adeniran G. A.(2015c). Mathematical Analysis of Diarrhea in the Presence of Vaccine. .*International Journal of Scientific and Engineering Research.* 6(12):396-404.

Adewale S. O., Olopade I. A., Ajao S. O., & Mohammed I. T. (2016a). Mathematical Analysis of Sensitive Parameters on the Dynamical Spread of HIV.*International Journal of Innovative Research in Science, Engineering and Technology.* 5(5): 2624-2635.

Adewale S. O., Olopade I. A.,Ajao S. O. & Adeniran, G. A. (2016b). Optimal Control Analysis of The Dynamical Spread Of Measles.*International Journal of Research GRANTHAALAYAH*. 4(5): 169-188.

Adler H., Gould S., Hine P., Snell L. B., Wong W., &Houlihan C. F. (2022). Clinical features and management of human monkeypox: a retrospective observational study in the UK. Lancet Infectious Diseases. DOI: http://dx.doi.org/10.1016/S1473-3099(22)00228-6

AjaoS. O., OlopadeI. A.,Akinwumi T. O., Adewale S. O., & Adesanya A. O. (2023).Understanding the Transmission Dynamics and Control of HIV Infection: A Mathematical Model Approach. *Journal of the Nigerian Society of Physical Sciences*. *5*(2).

Akinola E.I. Awoyemi B. E., Olopade I. A.,Falowo O. D., &Akinwumi T.O. (2021)Mathematical Analyssis of Diarrhea Model in the Presence of Vaccination and Treatment Waves with Sensitivity Analysis. *Journal of Applied Science and Environmental Management.* 25(7): 1077-1084.

Akinwumi T. O., OlopadeI. A.,Adesanya A. O., & Alabi M. O. (2021). Mathematical Model for the Transmission of HIV/AIDS with Early Treatment. *Journal of Advances in Mathematics and Computer Science*. 36(5): 35-51.

Bankuru S. V., Kossol S., Hou W., Mahmoudi P., Rychtář J., &Taylor D. (2020). A game-theoretic model of monkeypox to assess vaccination strategies. *PeerJ*. 8:e9272.

Bhunu C., Garira W., &Magombedze G. (2009) Mathematical analysis of a two strain hiv/aids model with antiretroviral treatment. *Acta Biotheor.* 57(3):361–381.

Bhunu C., &Mushayabasa S. (2011). Modelling the transmission dynamics of pox-like infections. *IAENG Int J*. 41(2):1–9

Brown K., &Leggat P. A. (2016). Human Monkeypox: Current State of Knowledge and Implications for the Future. *Trop Med Infect Dis*. 1(1).DOI:doi.org/10.3390/ tropicalmed1010008.

Bunge E. M., Hoet B., Chen L., Lienert F., Weidenthaler H., &Baer L. R. (2022). The changing epidemiology of human monkeypox: A potential threat? A systematic review. *PLoSNegl Trop Dis.* 16(2):e0010141. DOI:https://journals.plos.org/plosntds/ article?id=10.1371/journal.pntd.0010141

Castillo-Chavez C.,& Song B. (2004). Dynamical models of tuberculosis and their applications. *Math Biosci Eng* 1(2).

Centers for Disease Control and Prevention (CDC). Multistate outbreak of monkeypox--Illinois, Indiana, and Wisconsin. (2003). MMWR Morb Mortal Wkly Rep 13; 52(23) :37–40. Available from: https://www.ncbi.nlm.nih.gov/pubmed/12803191.

Doty J. B., Malekani J., Kalemba L., Stanley W. T., Monroe B. P., Nakazawa Y. U., & Karem K. L., (2017). Assessing Monkeypox virus prevalence in small mammals at the human–animal interface in the Democratic Republic of the Congo. *Viruses*. 9(10) 283. DOI: 10.3390/v9100283.

Hoff N. A., Doshi R. H., Colwell B., Kebela-Illunga B., Mukadi P., &Mossoko M. (2017). Evolution of a Disease Surveillance System: An Increase in Reporting of Human Monkeypox Disease in the Democratic Republic of the Congo, 2001-2013. Int J Trop Dis Health25(2). DOI: http://dx.doi.org/10.9734/IJTDH/2017/35885

Jezek Z., Grab B., Szczeniowski M. V., Paluku K. M., &Mutombo M. (1988). Human monkeypox: secondary attack rates. *Bull World Health Organ*. 66(4): 65–70.

Larkin M. (2003). Monkeypox spreads as US public-health system plays catch-up. *Lancet Infect Dis*. 3(8):461. DOI:http://dx.doi.org/10.1016/s1473-3099(03)00713-8

Markewitz N. F., DeLuca J., Kalejaiye A., Shidid S., Jain T., &Parikh P. (2023). Mpox-Associated Pneumonia: A Case Report. *AIM Clinical Cases*. 2(3):e220945. DOI: https://doi. org/10.7326/aimcc.2022.0945

Mitjà O., Alemany A., Marks M., Lezama J. I., Rodríguez-Aldama J. C.,& Torres M. S. (2023) Mpox in people with advanced HIV infection: a global case series. DOI: http://dx.doi.org/10.1016/S0140-6736(23)00273-8

Nguyen MT, Mentredy A, Schallhorn J, Chan M, Aung S, Doernberg S. B (2023). Isolated Ocular Mpox without Skin Lesions, United States. *Emerg Infect Dis*. 29(6). DOI: http:// dx.doi.org/10.3201/eid2906.230032

Nguyen P., Ajisegiri W., Costantino V., Chughtai A., &Maclntyre C. (2021). Reemergence of human monkeypox and declining population immunity in the context of urbanization, Nigeria, 2017–2020. *Emerg Infect Dis*. 27(4):1007–1014.

Olopade I. A., Adesanya A. O.& Mohammed I. T. (2017). Mathematical Analysis of the Global Dynamics of an SVEIR Epidemic Model with Herd Immunity. *International Journal of Science and Engineering Investigations.* (IJSEI).6(69):141-148.

Olopade I. A., Adesanya A. O.&Akinwumi T. O. (2021a). Mathematical Transmission of SEIR Epidemic Model with Natural Immunity.*Asian Journal of Pure and Applied Mathematics.* 3(1):19-29.

Olopade I. A., Adewale S. O., MohammedI. T., Adeniran G. A., Ajao S. O.& Ogunsola A. W. (2021b). Effect of Effective Contact Tracing in Curtaining the Spread of Covid-19. *Asian Journal of Research in Biosciences*. *3*(2):118-134.

Olopade I. A., Adewale S. O., MohammedI. T., Ajao S. O., &Oyedemi O. T. (2016). Mathematical Analysis of the Role of Detection in the Dynamical Spread of HIV-TB Co-infection. *Journal of Advances in Mathematics.* 11(10): 5715-5740.

Olopade I. A., Ajao S. O., Adeniran G. A., Adamu A. K., Adewale S. O., &Aderele O. R. 2022. Mathematical Transmission of Tuberculosis (TB) with Detection of Infected Undetectected. *Asian Journal of Research in Medicine and Medical Sciences*. *4*(1): 100- 119.

Olopade I. A., Akinola E. I., Philemon M. E., Mohammed I. T., Ajao S. O., Sangoniyi S. O.,Adeniran G. A. (2024). Modeling the Mathematical Transmission of a Pneumonia Epidemic Model with Awareness. *J. Appl. Sci. Environ. Manage*. 28(2): 403-413.

Peter O., Viriyapong R., Oguntolu F., Yosyingyong P., Edogbanya H., &MO A. (2020). Stability and optimal control analysis of anscir epidemic model. J Math Comput Sci 2020(1):2722–2753.

Philemon M. E., Olopade I. A., &Ogbaji E. O. (2023). Mathematical Analysis of the Effect of Quarantine on the Dynamical Transmission of Monkey-Pox. *Asian Journal of Pure and Applied Mathematics*. 5(1): 473–492.

Priyamvada L., Carson W. C., Ortega E., Navarra T., Tran S., &Smith T. G. (2022). Serological responses to the MVA-based JYNNEOS monkeypox vaccine in a cohort of participants from the Democratic Republic of Congo. *Vaccine*.40(50):732.1–7. DOI: http://dx.doi.org/10.1016/j. vaccine.2022.10.078

Somma S., Akinwande N.,& Chado U. (2019). A mathematical model of monkey pox virus transmission dynamics. *IFE J Sci*. 21(1):195–204.

TeWinkel R. E. (2019). Stability analysis for the equilibria of a monkeypox model. Thesis and Dissertations: University of Wisconsin. https://dc.uwm.edu/etd/2132

Usman S. & Isa Adamu I. (2017). Modeling the Transmission Dynamics of the Monkeypox Virus Infection with Treatment and Vaccination Interventions. *Journal of Applied Mathematics and Physics*, 5, 2335-2353. DOI: 10.4236/jamp.2017.512191.

World Health Organization. Fact sheet: Mpox. Available from: https://www.who.int/news-room/fact-sheets/detail/monkeypox